Aluminum under high pressure. II. Resistivity*

J. Cheung and N. W. Ashcroft
Laboratory of Atomic and Solid State Physics, Cornell University, Ithaca, New York 14853
(Received 22 February 1979)

The scaled room-temperature resistivity $[\rho(p)/\rho(p=0)]$ of crystalline aluminum is calculated as a function of pressure p. Initially the resistivity is determined as a function of volume from the standard variational treatment in which the required electron levels and distortions to the Fermi surface are described in a two-plane-wave model. To obtain the resistivity as a function of pressure, the results of this calculation are combined with a previously computed equation of state aluminum. The calculated scaled resistivity then shows a minimum at a pressure of about 25 GPa. This minimum is largely attributable to the increasing importance of distortions of the actual Fermi surface as pressure increases.

I. INTRODUCTION

The electronic structure of aluminum is relatively simple. Its bands have a largely free-electron-like character and can be interpolated quite accurately by a spatially local pseudopotential. On the other hand its Fermi surface is a complex multiply connected object that is sensitive to the choice of the pseudopotential components used to interpolate the band structure. Since the transport coefficients, and in particular the resistivity, are related to integrals over the Fermi surface, one might expect this sensitivity to become apparent if, as through the application of pressure, the pseudopotential coefficients are altered. As we shall see below, this is indeed partly the case, though in crystalline aluminum the pressure dependence of resistivity turns out to be an aggregate of some partially compensating effects. This compensation is very much a property of the metal itself (in Pb, for example, the effects we discuss should be more prominent) and also of its state (in solid aluminum the effects are far more noticeable than in the liquid state[1]).

We are concerned in this paper (as in Ref. 1) with the scaled room-temperature resistivity $\rho(p)/\rho(p=0)$ of crystalline Al, at a pressure p. The natural quantity to calculate is the ratio $\rho(V)/\rho(V_0)$, where V is the volume of a sample at pressure p (and V_0 its value at $p=0$). The starting point of this calculation is the well-known variational expression[2] for a bound on $\rho(V)$, as described in Sec. II. For metals with complicated Fermi surfaces, the necessary computations generally require numerical procedures of matching complexity, even for relatively simple choices of the variational trial function. The result for $\rho(V)$ can certainly be expected to depend on this choice as well as on approximations made necessary for wholly numerical reasons. Much of the consequent uncertainty can, however, be reduced by focusing attention on the scaled quantity $\rho(V)/\rho(V_0)$ and, as discussed in Sec. II, it is largely for this reason that we find it convenient to use the simplest form of trial function. Within this approximation it still remains to determine the behavior of the pseudopotential v_p, the band structure, and the Fermi surface as functions of volume. This is described in Sec. III. The piecewise two-plane-wave approximation that we use in evaluating the variational integrals is described in Sec. IV. The matrix elements appearing in the integrand also require the phonon frequencies and their volume dependences, a question that is taken up both in Secs. IV and V. The additional approximations we make in order to complete the numerical procedures are described in more detail in Sec. IV. They involve certain simplifications in the Fermi-surface geometry and in the description of the electronic levels associated with that geometry. The results are discussed in Sec. VI.

The calculations we report could be performed in principle for all simple metals. We have selected aluminum for the reasons given earlier,[3] namely that its high electron density and small ion core imply an ability to sustain a high pressure without core contact. In addition, the equation of state of Al has been calculated to pressures in excess of 300 GPa (3 Mbar). This information allows us to convert from $\rho(V)/\rho(V_0)$ to $\rho(p)/\rho(p=0)$ and hence arrive at the curves described in Sec. V.

II. RESISTIVITY OF SIMPLE METALS

For a metal of valence Z, the standard variational reduction of the Boltzmann equation yields for the resistivity at high temperatures the expression[2]

$$\rho \lesssim \frac{a_0\hbar}{e^2}\,\frac{2\pi Z}{a_0 k_F}\,\frac{\frac{2}{9}\pi}{\left[\int d^2x/v/v_p(\hat{\mathbf{v}}/v_F)\Phi(x)\right]^2}\,2\beta\mathcal{E}_F\frac{m}{M}I\,, \tag{1}$$

where

$$I=\int \frac{d^2x_1}{v_1/v_F}\int \frac{d^2x_2}{v_2/v_F}[\Phi(\vec{x}_2)-\Phi(\vec{x}_1)]^2 \times\sum_\lambda \frac{|\hat{\epsilon}_\lambda(\vec{x}_2-\vec{x}_1)\cdot\langle\vec{x}_2|\nabla w|\vec{x}_1\rangle|^2}{\sinh^2[\frac{1}{2}\beta\hbar\omega_\lambda(\vec{x}_2-\vec{x}_1)]}\,.$$

Here Φ is the trial function used in obtaining the bound for ρ, k_F is the magnitude of the Fermi wave vector, v_F is the Fermi velocity, $\mathcal{E}_F$ is the Fermi energy, $\beta=1/k_BT$, M is the mass of an ion, and ω_λ and $\hat{\epsilon}_\lambda$ refer to the frequency and polarization of phonons with reduced wave vector $\vec{x}$. We use scaled wave vectors $\vec{x}=\vec{k}/2k_F$ and a scaled pseudopotential $w=v_p/\frac{2}{3}\mathcal{E}_F$, where $-\frac{2}{3}\mathcal{E}_F$ is the known long-wavelength limit of the pseudopotential form factor. The quantity $a_0\hbar/e^2$ is the atomic unit of resistivity and has the value 21.7 $\mu\Omega$ cm.

In the one-plane-wave approximation the quantity I in (1) can be written

$$2\beta\mathcal{E}_F\frac{m}{M}I=\int \frac{d^2x_1}{v_1/v_F}\int \frac{d^2x_2}{v_2/v_F}[\Phi(\vec{x}_2)-\Phi(\vec{x}_1)]^2 \times|w(\vec{x}_2-\vec{x}_1)|^2S(\vec{x}_1,\vec{x}), \quad (2)$$

where $S(\vec{x}_1,\vec{x}_2)$ is the one-phonon structure which takes the form

$$S(\vec{x})=S(\vec{x}_2-\vec{x}_1)=2\beta\mathcal{E}_F\frac{m}{M}\sum_\lambda[\hat{\epsilon}_\lambda(\vec{x})\cdot\vec{x}]^2 \times\sinh^2[\tfrac{1}{2}\beta\hbar\omega_\lambda(\vec{x})]. \quad (3)$$

The sum in (3) is over the possible polarizations λ, and the integral is over the actual Fermi surface which in the case of the alkali metals, for example, can be very well approximated by a sphere. For the polyvalent metals, however, the shape of the Fermi surface must be taken into account since a substantial fraction of the free-electron Fermi surface can actually be lost.

It has been shown[4,5] that for the calculation of high-temperature resistivity the effects of anisotropy in the choice of trial functions are of diminishing importance. As a consequence of this observation we have used a trial function of the form

$$\Phi(\vec{x})\propto\vec{v}(\vec{x})\cdot\hat{z}\,, \quad (4)$$

(where $\hat{z}$ is parallel to the electric field) recognizing that although the calculated resistivity must necessarily be in excess of the actual value, the effect of the approximation on $\rho(p)/\rho(0)$, as noted earlier, will be much reduced. Although this choice for Φ greatly simplifies the numerical work, a generalization to more complex forms for Φ is quite straightforward.

Given (4) as the trial function then for a cubic system, (1) becomes

$$\rho\lesssim\frac{a_0\hbar}{e^2}\frac{2\pi Z}{a_0k_F}\left(\frac{m_{\rm opt}}{m}\right)^2 2\beta\mathcal{E}_F\frac{m}{M}I\,, \quad (5)$$

where

$$\frac{m}{m_{\rm opt}}=\frac{\int ds_{\vec{k}}\,v(\vec{k})}{s_0v_F} \quad (6)$$

defines the optical effective mass which can be calculated directly.[6] In (6) s_0 is the area of the free-electron Fermi surface ($s_0=4\pi k_F^2$). Attention then reverts to the remaining double surface integral in I, which we shall treat in a two-plane-wave approximation. Were the Fermi surface spherical, a one-plane-wave treatment would suffice and the identity

$$\int_{s_F}ds_{\vec{k}}\int_{s_F}ds_{\vec{k}'} =\int d\vec{k}\int d\vec{k}'\,\delta(k-k_F)\delta(k'-k_F) \quad (7)$$

reduces the problem to a single volume integral over $\vec{q}=\vec{k}-\vec{k}'$. With these simplifying features the calculation of the resistivity in the alkali metals is itself relatively simple. In the polyvalent metals, however, transformation (7) will not correctly treat transitions involving parts of the Fermi surface that depart from a simple spherical character. On the other hand (as we shall see) there *are* portions of the actual Fermi surface that remain very spherical and contributions from these can be transformed into a corresponding volume integral. The remaining (nonspherical) portions must, however, be treated by evaluating (1) directly.

III. PSEUDOPOTENTIAL AND FERMI-SURFACE GEOMETRY

In the two-plane-wave approximation to be discussed in Sec. IV, the electronic energy $\mathcal{E}$ for level k is given near zone planes by the solutions of

$$\begin{vmatrix}\mathcal{E}_{\vec{k}}-\mathcal{E} & V_p(\vec{K})\\ V_p(\vec{K}) & \mathcal{E}_{\vec{k}-\vec{K}}-\mathcal{E}\end{vmatrix}=0\,, \quad (8)$$

where $\vec{K}$ is the reciprocal-lattice vector under consideration and $\mathcal{E}_{\vec{k}}=(\hbar^2/2m)k^2$. $V_p(\vec{K})$ is related to the screened pseudopotential $v_p(\vec{K})$ by $V_p(\vec{K})=\Omega_0^{-1}v_p(\vec{K})$, where Ω_0 is the volume of the primitive cell: by choice $V_p(0)=0$.

In order to calculate the resistivity we need to know the form of the pseudopotential $v_p(k)$ throughout the range $0\leq k\leq 2k_F$. For aluminum, a one-parameter empty-core potential serves adequately.[7] In $\vec{k}$ space it can be written (with $x=k/2k_F$ and $s=2k_Fr_c$)

$$v_p(\vec{x})=\frac{-\pi Ze^2}{x^2k_F^2\epsilon(x)}\cos(sx)\,. \quad (9)$$

Here r_c is the parameter usually referred to as

the "empty-core radius." The value of r_c should be close to the size of the ion core on physical grounds and is around $1.12a_0$ for aluminum. For the dielectric function $\epsilon(x)$, we take[8]

$$\epsilon(x) = 1 + H(x)[1 - G(x)],$$

with

$$H(x) = (\pi a_0 k_F x^2)^{-1}\left(\frac{1}{2} + \frac{1-x^2}{4x}\ln\left|\frac{1+x}{1-x}\right|\right) \qquad (10)$$

and

$$G(x) = x^2/(2x^2+\xi).$$

The exchange-correlation parameter ξ is given by[8]

$$\xi = 1/(1+\alpha r_s),$$

where r_s is the electron spacing radius defined by $\Omega = \frac{4}{3}\pi Z r_s^3$, and $\alpha \cong 0.025$.

The screened pseudopotential form factor for aluminum is plotted in Fig. 1. In the same figure we also show the corresponding quantity for the compressed metal with $V/V_0 = 0.7$. On plotting w as a function of x we see that the node (where $w = 0$) moves to lower reduced wave vector as the metal is compressed. Correspondingly the Fourier coefficients $V_p(111)$ and $V_p(200)$ are seen to increase. While pseudopotential theory suggests that r_c should be energy dependent,[9] the energy dependence is expected to be small since r_c reflects the size of the ion core which should not change greatly with pressure-induced changes in its environment. Holding r_c fixed is tantamount to ignoring such small additional energy dependence.

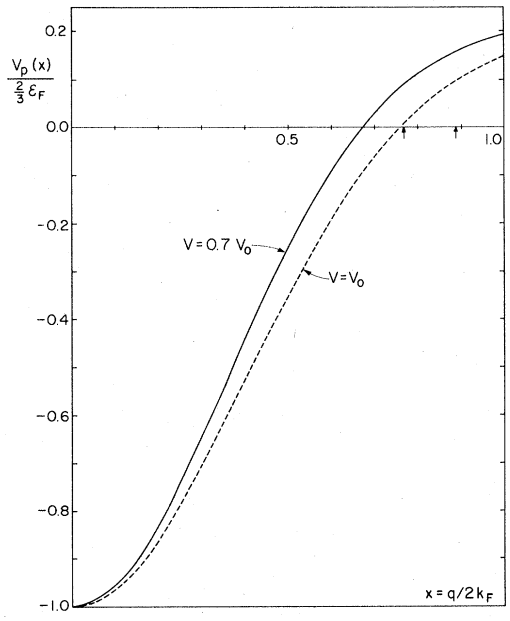

FIG. 1. Pseudopotential form factor of aluminum for $V/V_0 = 1.0$ and $V/V_0 = 0.7$. Screening by conduction electrons [Eq. (10)] the appropriate densities is taken into account. the empty-core radius r_c is $1.12a_0$. The arrows mark the location of the reciprocal-lattice vectors K = (1, 1, 1) and (2, 0, 0).

With the "new" values of $V_p(111)$ and $V_p(200)$ (for the compressed metal) we can use (8) again to map out the Fermi surface. Because of the different values of the new Fourier coefficients, the geometry of the Fermi surface of the compressed metal can be different from that of the metal under normal conditions. We take this into consideration.

IV. TWO-PLANE-WAVE APPROXIMATION

The evaluation of the double surface integral in (1) has been a major numerical obstacle in most of the calculations of the resistivity of polyvalent metals. Because of the complex geometry of the Fermi suface of these metals a large number of surface-area elements is necessary to characterize the surface accurately.[10-12] For the high-temperature transport coefficients the problem of the Fermi-surface anisotropy is less,[4,5] and in view of this we have chosen to carry out the calculations by means of a two-plane-wave approximation which has also been used by other authors in similar model calculations.[13,14] Although at some points on the Fermi surface three or even four orthogonalized plane waves are needed to give an adequate description of the finer distortions,[15] the amount of surface requiring this more detailed description is small compared with the total Fermi-surface area. Essentially, our approximation treats each of the many Bragg planes in turn and calculates the contribution to the resistivity with the electronic levels described by the linear combination of plane waves

$$\Psi_{\vec{k}}(\vec{r}) = \sin\theta_{\vec{k}} e^{i\vec{k}\cdot\vec{r}} + \cos\theta_{\vec{k}} e^{i(\vec{k}-\vec{K})\cdot\vec{r}}. \qquad (11)$$

The total resistivity is then the sum of the umklapp contributions of the individual reciprocal-lattice vector ($\vec{K}$) and the normal contribution. Our numerical calculations show that the normal contribution is only a small part of the total resistivity and for this it is quite adequate to use the simple one-plane-wave treatment.

Consider the umklapp processes made possible by transitions involving a particular reciprocal-lattice vector $\vec{K}$. The umklapp processes are those for which the initial levels $\vec{k}_1$ originate on the Fermi surface and the final levels $\vec{k}_2$ end on the remapped surfaces, i.e.,

$$\vec{k}_2 - \vec{k}_1 = \vec{q} - \vec{K} \qquad (12)$$

with $\vec{q}$ in the first Brillouin zone. Some umklapp

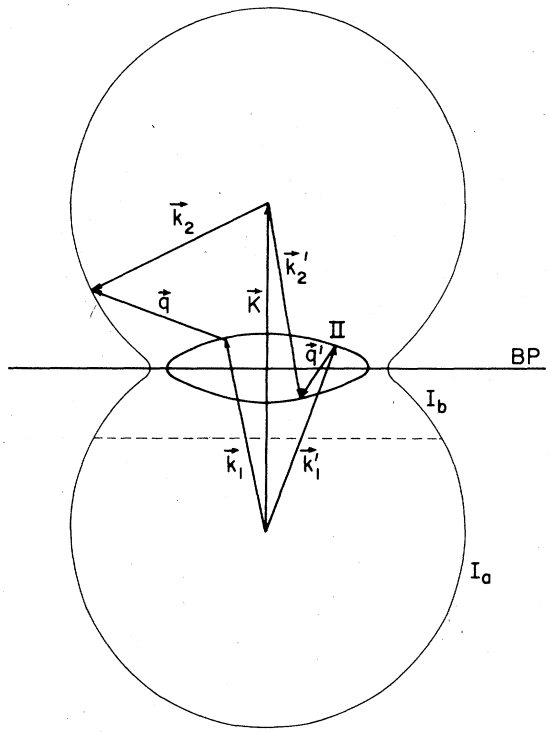

FIG. 2. Two possible umklapp processes are shown here in the single-Bragg-plane (BP) approximation ($\vec{k}_1 \rightarrow \vec{k}_2$; $\vec{k}_1' \rightarrow \vec{k}_2'$). Note that the Fermi surface is divided up into three parts for computational purposes as described in the text.

processes are pictured in Fig. 2 where we also see that the Fermi surface is split into two sections because of the finite value of $v_{\vec{K}}$.

The parameter θ describing the electron levels in (11) is given by

$$\tan\theta_{\vec{k}} = \eta \pm \mathrm{sgn}(v_{\vec{K}})(\eta^2+1)^{1/2},$$

with

$$\eta = [4\mathcal{E}_F/|V_p(\vec{K})|] \times [\hat{x}\cdot(\vec{K}/2k_F) - \tfrac{1}{2}(K/2k_F)^2], \quad x = k/2k_F. \tag{13}$$

The ($\pm$) in (13) signify the band index, with (+) for the second band and (–) for the first.

The matrix element M required in (1) is in general given by

$$-i\hat{e}_\lambda(\vec{x}_2 - \vec{x}_1)\cdot\langle \vec{x}_2|\vec{\nabla}w|\vec{x}_1\rangle$$

when the wave functions are normalized. Before we consider this further we will first describe the approximations we make concerning the phonon frequencies and polarizations. With the exception of those along the major symmetry axes, the phonons have polarizations that are neither pure longitudinal nor pure transverse. However, the large number of symmetry axes present in the Brillouin zone of the cubic structures guarantees that throughout the zone the phonons have polarizations that are usually quite close to being purely longitudinal or purely transverse. It thus seems reasonable to replace the phonon dispersion curves with one longitudinal branch and two identical transverse branches with dependence on the magnitude of $\vec{q}$ alone, these branches being appropriately weighted averages of the frequencies along the major symmetry axes. Implicit in this is the subsequent replacement of the zone by the Debye sphere. The individual phonon frequencies are calculated from an eight-shell axially symmetric model with *experimental force-constants* obtained from experiments at 300 °K.[16] This procedure inevitably introduces errors into the final result, but the uncertainties are not expected to be large, especially if the main interest centers on the way resistivity changes as a consequence of the *variation* of the frequencies themselves.

With this approximation, the scaled longitudinal and transverse matrix elements (squared) are then given by

$$(2k_F)^2(\tfrac{2}{3}\mathcal{E}_F)^2 M_L^2(\vec{k}_2,\vec{k}_1) = \{q\,V_p(\vec{q})(S_1S_2 + C_1C_2) + q\,V_p(\vec{q}-\vec{K})S_2C_1 + q\,V_p(\vec{q}+\vec{K})S_1C_2 + \hat{q}\cdot\vec{K}[V_p(\vec{q}+\vec{K})S_1C_2 - V_p(\vec{q}-\vec{K})S_2C_1]^2\}^{1/2} \tag{14}$$

and

$$(2k_F)^2(\tfrac{2}{3}\mathcal{E}_F)^2 \sum_T M_T^2(\vec{k}_2,\vec{k}_1) = K^2[1-(\hat{q}\cdot\hat{K})^2][V_p(\vec{q}+\vec{K})S_1C_2 - V_p(\vec{q}-\vec{K})S_2C_1]^2,$$

where $S_i = \sin\theta_i$ and $C_i = \cos\theta_i$ with $i = 1, 2$. Given the trial function (4) the quantity $[\Phi(k_2) - \Phi(k_1)]^2$ appearing in (1) is determined by

$$(2k_F)^2[\Phi(\vec{k}_2) - \Phi(\vec{k}_1)]^2 = q^2 + 2\vec{q}\cdot\vec{K}(C_1^2 - C_2^2) + K^2(C_2^2 - C_1^2)^2. \tag{15}$$

If the band gaps are small (as in aluminum) then only a small region of the Fermi sphere needs to be described in the two-plane-wave formalism, the rest being essentially free-electron-like. Considerable computational effort can be saved if we divide up the first band into two parts (see Fig. 2), I_a and I_b, in which I_a is the part of the first band where a one-plane-wave description would be adequate while I_b is the part that requires the two-plane-wave description (as determined by a suitably chosen criterion[17]). The processes involving initial states on I_a and final states on the remapped part of I_a are essentially free-electron-like and

will be dealt with separately. Contributions from processes involving II and I_b will then be computed by directly evaluating the double integral.

The double Fermi-surface integrals required for the evaluation of (1) thus have contributions from the normal processes (which are small in the case of aluminum), umklapp processes in the two-plane-wave single-Bragg-plane approximation, and umklapp processes that can be considered as involving free-electron-like levels.

V. APPLICATION TO COMPRESSED ALUMINUM

As mentioned above, the phonon frequencies at normal conditions (300 °K and zero pressure) are generated by an axially symmetric force-constant model. The effects of the volume change on the phonon frequencies themselves) can be calculated in a straightforward manner from the dynamical matrices.[18,19] In the polyvalent metals it is well known that such a calculation is computationally time consuming as a large number of terms is needed for the dynamical matrices to converge. We choose instead to scale all the frequencies with the bulk experimental Grüneisen parameter γ (2.35 for aluminum[20]), i.e.,

$$\omega(q, v) = \omega_0(q)\left(1 + \gamma \frac{V_0 - V}{V}\right). \tag{16}$$

In (16) $\omega(q, V)$ is the phonon frequency of the wave vector q at the compressed volume V and ω_0 is the observed frequency at the zero-pressure volume V_0. Though a crude approximation for the changes in the frequencies themselves, it should be satisfactory for the quotient $\rho(V)/\rho(V_0)$ involving ratios of integrals accompanying such changes. A more realistic approach is to take into account the changes in the elastic constants in the evaluation of the changes in the phonon frequencies.[21]

The numerical evaluation of Eq. (1) also involves the computation of the factor $(m_{\text{opt}}/m)^2$. From Eq. (6) we see that this factor is a measure of the distortions in the Fermi surface. On the other hand, we note that in evaluating the umklapp contributions to the double surface integral, the Fermi surface used is *not* the actual fully distorted Fermi surface. For each particular Bragg plane (at, say, $\frac{1}{2}\vec{K}$) only the distortions associated with a given $V_p(\vec{K})$ are taken into account. This amounts to using a Fermi surface with an area *larger* than the actual one (in our two-plane-wave model, the actual Fermi surface would have distortions resulting from 14 Bragg planes). We can estimate the combined effects of the necessary further *reduction* in Fermi-surface area as follows.[22] We note that, with the trial function given by (4), the double surface integral in (1) takes the form

$$\int \frac{ds_1}{v_1} \int \frac{ds_2}{v_2} |\vec{v}_2 - \vec{v}_1|^2 \ldots , \tag{17}$$

where the rest of the integrand has a somewhat weaker dependence on the location on the Fermi surface. The ratio of

$$\int \frac{ds_1}{v_1} \int \frac{ds_2}{v_2} |\vec{v}_2 - \vec{v}_1|^2$$

to a corresponding quantity for the free-electron case is thus an approximation of the correction factor required. Using inversion symmetry, we have

$$\frac{\int (ds_1/v_1) \int (ds_2/v_2) |\vec{v}_2 - \vec{v}_1|^2}{\int (ds_1^0/v_1^0) \int (ds_2^0/v_2^0) |\vec{v}_2^0 - \vec{v}_1^0|^2} = \frac{\int (ds/v) \int ds v}{\int (ds^0/v^0) \int ds^0 v^0} , \tag{18}$$

where $\int ds\, v / \int ds^0\, v^0$ is just m/m_{opt} while $(\int ds/v)/(\int ds^0/v^0)$ is commonly referred to as the specific-heat effective mass m_{sh}/m. Combining this with the factor $(m_{\text{opt}}/m)^2$, we arrive at a total correction factor $f = (m_{\text{opt}}/m)(m_{\text{sh}}/m)$. In the two-plane-wave model m_{opt} and m_{sh} can be obtained without further approximation in closed form[6]:

$$\frac{m}{m_{\text{opt}}} = 1 - \sum_K \frac{1}{2} \frac{K}{2k_F} \frac{|V_p(K)|}{\mathcal{E}_F} \left\{ \left[\frac{\pi}{2} - \sin^{-1}\left(\frac{2V_p(K)}{\omega_0}\right)\right] + \frac{|V_p(K)|}{2\mathcal{E}_K} \left[\frac{\omega_0}{2\omega_1} + \frac{3\omega_1}{2\omega_0} - 2 - \ln\left(\frac{\omega_1}{\omega_0}\right)\right]\right\},$$

where

$$\omega_0 = 2[\mathcal{E}_K \mathcal{E}_F + V_p^2(K)]^{1/2} - \mathcal{E}_K \tag{19}$$

and

$$\omega_1 = 2[\mathcal{E}_K \mathcal{E}_F + V_p^2(K)]^{1/2} + \mathcal{E}_K .$$

Further,

$$\frac{m_{\text{sh}}}{m} = 1 - \frac{1}{2} \sum_K (1 - X - \{1 + X^2 - [4X^2 + \tfrac{9}{4}\omega^2(X)]^{1/2}\}^{1/2}),$$

where $X = K/2k_F$. These formulas then serve as an indication of the accuracy of our numerical procedure within the two-plane-wave model. The results are listed in Table I. We note also that the scaled correction factors, i.e., $f(r_s)/f(r_{s0})$, compare very well. The resistivity of aluminum as a function of compressed volume is plotted in Fig. 3. Here we display the results using both the correction factors from the closed form solutions (f_a) and those from the numerical calculations (f_n).

The equation of state of aluminum has been obtained by Friedli and Ashcroft.[3] They examined most of the common crystal structures and concluded that for the pressure range they considered (up to and above 300 GPa) the fcc structure is that of lowest calculated energy. We can numerically

TABLE I. Quantities m_{opt}/m and m_{sh}/m evaluated in the two-plane-wave model. Both closed-form (analytical) and numerical results are listed. The quantity f is defined by $f=(m_{opt}/m)(m_{sh}/m)$. (*Note*: $r_{s0}=2.073$.)

		m_{opt}/m		m_{sh}/m		$f(r_s)/f(r_{s0})$	
$r_s(a_o)$	V/V_o	Analytical	Numerical	Analytical	Numerical	Analytical	Numerical
2.073	1.00	1.370	1.305	0.985	0.987	1.00	1.00
2.001	0.90	1.644	1.561	0.976	0.979	1.19	1.18
1.924	0.80	2.070	1.910	0.964	0.966	1.48	1.43
1.841	0.70	2.819	2.552	0.947	0.949	1.98	1.88

eliminate r_s between this equation of state and the resistivity variation we obtain in this calculation to arrive at a scaled resistivity curve which is shown in Fig. 4. Unfortunately, we have not been able to locate experimental data on the pressure variation of the resistivity of crystalline aluminum. The data of Bridgman summarize the measurement of relative *resistance* rather than the relative resistivity.[23,24] However, we can get an estimate of the experimental value of

$$[\Delta(\rho/\rho_0)/\Delta(V/V_0)]_{V/V_0=1}$$

from the Bridgman data by using the approximate equation for an isotropic cubic crystal (roughly applicable to the experimental arrangement of Bridgman):

$$\left.\frac{\Delta(\rho/\rho_0)}{\Delta(V/V_0)}\right|_{V/V_0=1}=\left.\frac{\Delta(R/R_0)}{\Delta(V/V_0)}\right|_{V/V_0=1}+\frac{1}{3}. \tag{20}$$

With this equation we get 2.3 for the experimental value[25] of $\Delta(\rho/\rho_0)/\Delta(V/V_0)$ and this should be compared with the theoretical result of 2.5 obtained here.

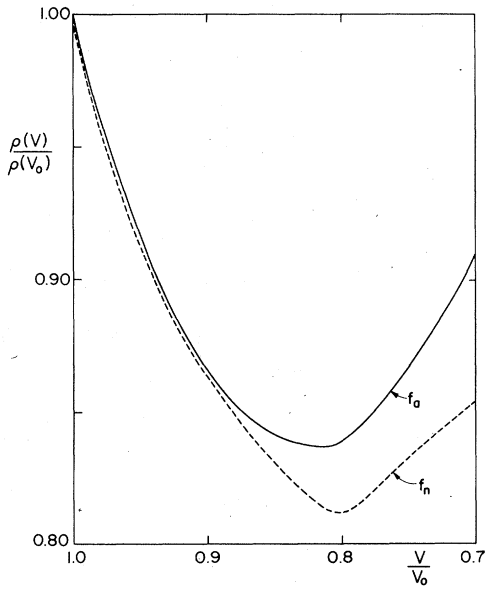

FIG. 3. Scaled resistivity of aluminum as a function of compressed volume at T = 300 °K in the single-Bragg-plane two-plane-wave approximation. The curve labeled f_a is obtained by applying the Fermi-surface-area correction factor in closed form: the f_n curve is obtained with the correction factor obtained numerically (see text).

VI. DISCUSSION AND CONCLUSION

Our calculations, though they describe quite well the qualitative trend of the behavior of resistivity under pressure (as compared with experiments at low pressures), do not yield particularly accurate numerical results for the resistivity itself. At normal conditions the resistivity $\rho(0)$ is overestimated by 50% (the computed values are 4.2 and 4.0

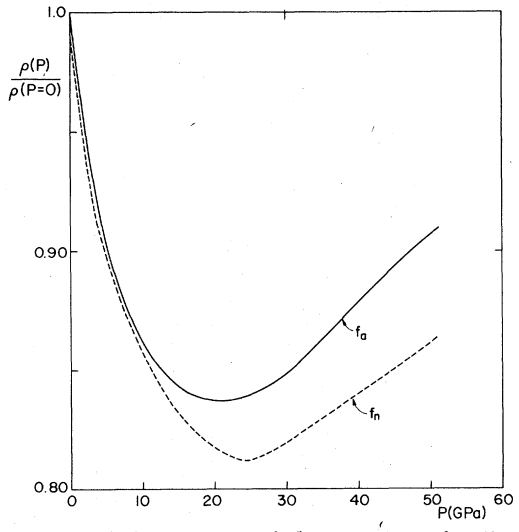

FIG. 4. Scaled resistivity of aluminum as a function of pressure. The curves are obtained by numerically eliminating the volume between the curves shown in Fig. 3 with the equation of state of aluminum. The equation of state is obtained by the procedure described in Ref. 3.

$\mu\Omega$ cm with the correction factors f_a and f_n, respectively) and is characteristic of the errors encountered in the equivalent calculation in the liquid state.[1] The discrepancy can be attributed to the approximations we have made and to the choice of trial function. The Fermi surface over which we perform our double surface integral is at best a rough approximation of the real Fermi surface which has a much more complex geometry. Our approximation of a single Bragg plane allows for more transitions to be included as the Fermi surface thus generated has a larger area than the real Fermi surface. This additional surface is only approximately accounted for in our treatment of applying the correction factor (18). Another source of error can be traced to the replacement of the phonon frequencies by three branches (one longitudinal and two identical transverse) and the replacement of the first Brillouin zone by a Debye sphere. This simplifies the problem but at the same time discounts all the effects of phonon anisotropy. The errors introduced by using a single Grüneisen parameter to describe the phonon frequency changes will be averaged out to a certain extent (at least for small volume changes) as an integral is performed to arrive at the resistivity. Furthermore, we note that the two-plane-wave approximation is not adequate for some electronic levels, especially those near the zone edges and corners. The electronic levels near the symmetry point W, for instance, require four plane waves for an adequate characterization. A realistic description of the electronic levels is attempted only near the Bragg plane under consideration—and this is only done crudely—a simplification that inevitably introduces errors into our results. We note, however, that the fraction of the Fermi surface that is close to a Bragg plane is already small. Thus, we can expect that the fraction that lies near the intersection of two or three of these Bragg planes to be smaller still. Further Bragg planes [the next class is (220)] are excluded from our consideration as they lie outside the Fermi sphere. The inadequacy of the trial function we use necessarily leads to overestimation of the resistivity.

However, we believe our results for the *scaled* quantity have quantitative validity in the description they give of the *changes* in the resistivity as pressure is applied, the previous objections notwithstanding. The reason is that when we consider the changes brought about by the application of pressure then the relative uncertainties in each of the considerations should be considerably reduced.

The results of our calculation are somewhat interesting in that the resistivity of aluminum shows a minimum as the metal is compressed. The mechanisms that cause this minimum are not the same as those believed to account for the resistivity minima in the alkali metals. In the latter case the admixture of d states in the levels at the Fermi energy is believed to be responsible,[23,26-29] while in the case of aluminum the minimum appears to be a manifestation of changes in the Fermic-surface geometry. In our simple model of the electron-ion pseudopotential under compression we see that for all the compressed volumes considered the reduced Fourier coefficients $v_p(111)/\mathcal{E}_F$ and $v_p(200)/\mathcal{E}_F$ *increase* as the metal is compressed. These increases cause the reduction in Fermi-surface area (as compared to the free-electron sphere) to increase from about 14% to about 38% when the volume of the sample is reduced by 30%. The values of the reduced Fourier coefficients and the Fermi surface area reductions are listed in Table II.

It is quite clear that a more careful treatment of the resistivity variation requires that the Fermi-surface distortions be *fully* taken into account. If the Fermi-surface effects are included (as described in Sec. V), we see that the simple picture of a one-plane-wave treatment needs to be modified. In addition to the (main) effect of reductions in resistivity stemming from increases in phonon frequencies[21] we have an offsetting effect from the increase in the distortions of the Fermi surface which ultimately reverses the trend. The net correction factor that should be applied for these distortions should be

$$f = (m_{\mathrm{opt}}/m)(m_{\mathrm{sh}}/m)$$

instead of the $(m_{\mathrm{opt}}/m)^2$ appearing in Eq. (1) because of a corresponding reduction in the region of integration for the double surface integral in Eq. (1). As m_{sh}/m remains near unity for all the values of r_s considered. we see that the correction factor is reflected by the increase (as a function of compression) of the optical mass. The two effects together cause a resistivity minimum at $V/V_0 \cong 0.8$ which would be absent in the one-plane-wave treatment.

TABLE II. Reduced Fourier coefficient $v_p(111)/\frac{2}{3}\epsilon_F$ and $v_p(200)/\frac{2}{3}\epsilon_F$ and the reduction in Fermi-surface area as a function of compressed volume. The two-plane-wave model is used to compute the Fermi-surface (FS) area reductions.

$r_s(a_o)$	V/V_o	$v_p(111)/\frac{2}{3}\epsilon_F$	$v_p(200)/\frac{2}{3}\epsilon_F$	FS Reduction
2.073	1.00	0.0080	0.0949	14%
2.001	0.90	0.0322	0.1144	22%
1.924	0.80	0.0585	0.1350	29%
1.84	0.70	0.0870	0.1564	38%

While the validity of the simple one-plane-wave treatment can be justified for high temperatures and zero pressure, we have found that in dealing with the compressed metal a more realistic treatment taking into consideration the Fermi-surface distortions is plainly required. As discussed above, this differs from the situation in the alkali metals where the distortions in the Fermi surface are second-order effects. As another example of a polyvalent metal we may consider Pb whose Fourier coefficients (or rather their magnitudes) are expected to *decrease* as the metal is compressed.[30] Therefore, both the Fermi-surface distortion (as reflected in the optical mass) and the increase in phonon frequencies cause the resistivity to decrease as a function of pressure and we would expect the pressure coefficient of Pb to be larger than the result from a one-plane-wave calculation. Thus, for the polyvalent metals our single-Bragg-plane and two-plane-wave approximation is a first step in taking these distortions into account and already shows that among the simple metals some qualitatively different effects can be expected.

ACKNOWLEDGMENT

This research has been supported by the United States Army Research Office, Research Triangle Park, North Carolina, under Grant No. DAAG29-78-G-0040.

---

*See AIP document no. PAPS PRBMDO-20-2991-51 for a lengthier version of this paper which includes a more detailed explanation of the calculational procedures. Order by PAPS number and journal reference from the American Institute of Physics, Physics Auxilliary Publication Service, 335 East 45th Street, New York, New York 10017. The price is $1.50 for each microfiche (98 pages), or $5 for photocopies of up to 30 pages with $0.15 for each additional page over 30 pages. Air mail additional. Make checks payable to the American Institute of Physics.

[1]J. Cheung and N. W. Ashcroft, Phys. Rev. B 18, 559 (1978).
[2]J. M. Ziman, *Electrons and Phonons* (Oxford University, London, 1960).
[3]C. Friedli and N. W. Ashcroft, Phys. Rev. B 12, 5552 (1975).
[4]J. Black and D. L. Mills, Phys. Rev. B 9, 1458 (1974).
[5]J. W. Ekin and A. Bringer, Phys. Rev. B 7, 4468 (1973).
[6]N. W. Ashcroft and K. Sturm, Phys. Rev. B 3, 1398 (1971).
[7]N. W. Ashcroft, Phys. Lett. 23, 48 (1966).
[8]D. J. W. Geldart and S. H. Vosko, Can. J. Phys. 44, 2137 (1966); 45, 2229(E) (1966); D. C. Wallace, Phys. Rev. 182, 778 (1969).
[9]V. Heine, Solid State Phys. 24, 1 (1970).
[10]Y. Bergman, M. Kaveh, and N. Wiser, Phys. Rev. Lett. 32, 606 (1974).
[11]A. B. Meador and W. E. Lawrence, Phys. Rev. B 15, 1850 (1977).
[12]H. K. Leung, F. W. Kus, N. McKay, and J. P. Carbotte, Phys. Rev. B 16, 4358 (1977); H. K. Leung, J. P. Carbotte, D. W. Taylor, and C. R. Leavens, Can. J. Phys. 54, 1585 (1976).
[13]W. E. Lawrence and J. W. Wilkins, Phys. Rev. B 6, 4466 (1972).
[14]H. B. Huntington and W. C. Chan, Phys. Rev. B 12, 5423 (1975); W. C. Chan and H. B. Huntington, *ibid.* 12, 5441 (1975).
[15]N. W. Ashcroft, Philos. Mag. 8, 2055 (1963).
[16]G. Gilat and R. M. Nicklow, Phys. Rev. 143, 487 (1966).
[17]The criterion used is that the electron velocity (calculated in the approximation used) on I_a differs from v_F, the Fermi velocity, by less than 1%.
[18]D. C. Wallace, Phys. Rev. 187, 991 (1969).
[19]P. V. S. Rao, J. Phys. Chem. Solids 35, 669 (1974).
[20]V. P. Singh and M. P. Hemkar, J. Phys. F 7, 761 (1977). References for experimental results of the bulk Grüneisen parameter are cited in this work.
[21]Such a calculation was done for the alkali metals by M. Kaveh and N. Wiser [Phys. Rev. B 6, 3648 (1972)].
[22]These effects are also discussed in Refs. 13 and 14. The way we allow for the Fermi-surface distortions is different from that of Ref. 14. See also, N. W. Ashcroft, Phys. Rev. B 19, 4906 (1979).
[23]F. P. Bundy and H. M. Strong, Solid State Phys. 13, 81 (1962).
[24]P. W. Bridgman, *The Physics of High Pressure* (Bell, London, 1949).
[25]Data taken from Ref. 23.
[26]H. G. Drickamer, Solid State Phys. 17, 1 (1965).
[27]J. S. Dugdale, in *Advances in High Pressure Research*, edited by R. S. Bradley (Academic, London, 1969), Vol. 2, 101.
[28]N. H. March, in *Advances in High Pressure Research*, edited by R. S. Bradley (Academic, London, 1969), Vol. 3, p. 241.
[29]J. M. Dickey, A. Meyer, and W. H. Young, Proc. Phys. Soc. Lond. 92, 460 (1967).
[30]The pseudopotential for Pb is discussed, e.g., by M. L. Cohen and V. Heine [Solid State Phys. 24, 38 (1970)].